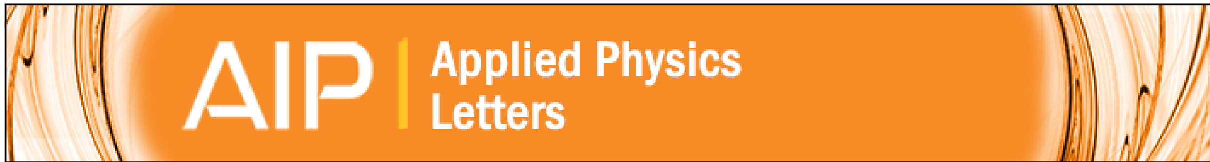

Effects of post-deposition annealing in O 2 on the electrical characteristics of LaAlO 3 films on Si

L. Miotti, K. P. Bastos, C. Driemeier, V. Edon, M. C. Hugon, B. Agius, and I. J. R. Baumvol

Citation: Applied Physics Letters **87**, 022901 (2005); doi: 10.1063/1.1989447
View online: http://dx.doi.org/10.1063/1.1989447
View Table of Contents: http://scitation.aip.org/content/aip/journal/apl/87/2?ver=pdfcov
Published by the AIP Publishing

Articles you may be interested in

Impact of post deposition annealing in the electrically active traps at the interface between Ge(001) substrates and LaGeOx films grown by molecular beam deposition
J. Appl. Phys. **110**, 084504 (2011); 10.1063/1.3651400

Impact of titanium addition on film characteristics of Hf O 2 gate dielectrics deposited by atomic layer deposition
J. Appl. Phys. **98**, 054104 (2005); 10.1063/1.2030407

Relationships among equivalent oxide thickness, nanochemistry, and nanostructure in atomic layer chemical-vapor-deposited Hf–O films on Si
J. Appl. Phys. **95**, 5042 (2004); 10.1063/1.1689752

Electrical properties of SrTiO 3 thin films on Si deposited by magnetron sputtering at low temperature
Appl. Phys. Lett. **79**, 1513 (2001); 10.1063/1.1398321

Interfacial silicon oxide formation during oxygen annealing of Ta 2 O 5 thin films on Si: Oxygen isotope labeling
J. Vac. Sci. Technol. A **18**, 2522 (2000); 10.1116/1.1286717

AIP Applied Physics Reviews
NEW Special Topic Sections
NOW ONLINE
Lithium Niobate Properties and Applications: Reviews of Emerging Trends
AIP Applied Physics Reviews

Reuse of AIP Publishing content is subject to the terms at: https://publishing.aip.org/authors/rights-and-permissions. Download to IP: 143.54.44.137 On: Thu, 05 May 2016 13:27:08

HTML ABSTRACT + LINKS

APPLIED PHYSICS LETTERS **87**, 022901 (2005)

Effects of post-deposition annealing in O_2 on the electrical characteristics of $LaAlO_3$ films on Si

L. Miotti,[a] K. P. Bastos, and C. Driemeier
Instituto de Física, Universidade Federal do Rio Grande do Sul, CP 15051, 91501-970 Porto Alegre, RS, Brazil

V. Edon, M. C. Hugon, and B. Agius
Laboratoire de Physique des Gaz et des Plasmas, Université Paris Sud, 91405 Orsay, France

I. J. R. Baumvol
Universidade de Caxias do Sul, CCET and Universidade Federal do Rio Grande do Sul, Porto Alegre, RS, Brazil

(Received 14 February 2005; accepted 6 June 2005; published online 5 July 2005)

$LaAlO_3$ films were deposited on *p*-type Si(100) by sputtering from a $LaAlO_3$ target. $C \times V$ characteristics were determined in nonannealed and O_2-annealed capacitors having $LaAlO_3$ films as dielectric and RuO_2 as top electrode. Thermal annealing in O_2 atmosphere reduced flat band voltage to acceptable values for advanced Si-based devices. ^{16}O–^{18}O isotopic substitution was characterized by Rutherford backscattering spectrometry and nuclear resonant reaction profiling. Chemical analysis of the films was accomplished by x-ray photoelectron spectroscopy. The electrical improvements observed after thermal annealing in O_2 were attributed to the incorporation of oxygen from the gas phase, possibly healing oxygen vacancies in the films and providing mobile oxygen to the interface. © *2005 American Institute of Physics*. [DOI: 10.1063/1.1989447]

In order to meet the required power consumption and reliability constrains, several materials holding a dielectric constant higher than that of SiO_2 ($\kappa \sim 3.9$) have been proposed as replacement for silicon oxide/oxinitride for gate dielectrics in ultralarge scale integration (ULSI) metal-oxide-semiconductor field effect transistor (MOSFET) device technology.[1–3]

Lanthanum oxide (La_2O_3) has been considered as a potential high-κ dielectric due to its high dielectric constant ($\kappa \sim 30$) as compared to SiO_2 and wide band gap ($\sim$5 eV).[1,4] However, during thermal annealing of La_2O_3 films on Si, most of the stability requirements are not fulfilled.[5–7] As an alternative, lanthanum aluminate ($LaAlO_3$) is expected to be more thermodynamically stable in contact with Si and may eventually meet thermal processing requirements, since the addition of Al raises the crystallization temperature and chemical stability of most high-κ materials studied so far.[3,8–10] Since the $LaAlO_3$ bulk dielectric constant and band gap (κ_{bulk}=20–25, band gap=5.6 eV) do not differ significantly from that of La_2O_3,[1,4] this material constitutes indeed a potential alternative for high-κ dielectric application. Although scarce, experimental investigation of $LaAlO_3$ films on Si has shown that, analogous to many other high-κ dielectrics on Si, post-deposition annealing (PDA) performed at various different temperatures is crucial to produce a gate stack with electrical characteristics within ULSI design specifications.[11]

This letter reports on the effects of PDA in O_2 atmosphere on the electrical, physicochemical and atomic transport characteristics of $LaAlO_3$ films deposited on Si. Lanthanum aluminate films 5–40 nm thick, as determined by x-ray reflectometry, were sputter deposited from a $LaAlO_3$ ceramic target in a 5×10^{-2} mbar Ar plasma excited by a 13.56 MHz radio frequency, on HF last *p*-type Si(100) wafers etched in a buffered (20%) HF solution for $\sim$30 s. The distance between the substrate and target was fixed at 9 cm and the plasma power at 1 W/cm^2. The gas flow rate in the deposition chamber was set to 150 sccm. As it is shown below, within experimental uncertainties the as-deposited $LaAlO_3$ films had a La/Al ratio equal to 1. *Ex situ* thermal annealing was performed in a Joule-effect heated furnace at 450 or 600 °C, for 30 min in 200 mbar of O_2. The used O_2 gas was enriched to 97% in the ^{18}O isotope, allowing to distinguish oxygen atoms previously existent in the films (mostly ^{16}O) from those incorporated from the annealing atmosphere (^{18}O). Metal-oxide-semiconductor (MOS) capacitors were prepared by depositing on the as-deposited $LaAlO_3$ films conducting RuO_2 electrodes through a shadow mask by reactive sputtering of a Ru target in Ar:O_2 atmosphere. RuO_2 was chosen as the top electrode because a flat band voltage of nearly zero is expected for ideal $RuO_2/LaAlO_3/p$-Si capacitors.[12] The electrodes top areas were 0.36 mm^2. An InGa backside contact was deposited in order to improve electrical contact.

Figure 1(a) shows the high frequency (1 MHz) $C \times V$ characteristics of MOS capacitors built up with 5 and 40 nm thick, as-deposited $LaAlO_3$ dielectrics film on Si, as well as of capacitors made with $LaAlO_3$ films annealed in O_2 in the above described conditions. The simulated curve was calculated assuming 5.0 eV as the RuO_2 work function. Figure 1(a) shows that the flat band voltage shift measured for the capacitor bearing an as-deposited $LaAlO_3$ film displays a high, negative flat band voltage, as reported previously,[5,11] indicating a high oxide charge density ($>10^{13}$ cm^{-2}). The strong flat band voltage shift reduction after thermal annealing in O_2 suggests that the oxide charges are possibly related to oxygen deficiencies in the $LaAlO_3$ matrix.[11] The hysteresis in the $C \times V$ curves indicate the presence of interfacial electronic traps and/or mobile charge in the oxide. Annealing the 5 nm MOS capacitors in O_2 leads to a reduction of the capacitance at accumulation regime, possibly by growing a lower-κ interfacial layer. This lower-k interfacial layer has a

[a]Present address: Av. Bento Gonçalves, 9500, Porto Alegre, RS C.P. 15051, 91509 900 Brazil; electronic mail: miotti@if.ufrgs.br

Reuse of AIP Publishing content is subject to the terms at: https://publishing.aip.org/authors/rights-and-permissions. Download to IP: 143.54.44.137 On: Thu, 05 May 2016 13:27:08

 © 2005 American Institute of Physics

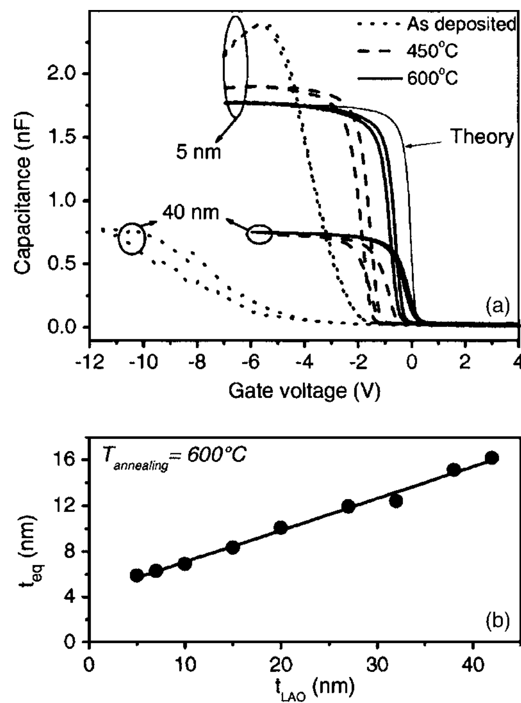

FIG. 1. (a) $C \times V$ Characteristics at 1 MHz of 5 and 40 nm as-deposited (dotted line) $LaAlO_3/Si$ films and O_2 annealed at 450 (dashed line) and 600 °C (solid line). RuO_2 top electrodes with 0.36 mm^2 area were used. The simulated curve for the 5 nm MOS capacitors is indicated. The $C \times V$ characteristics presents anticlockwise hysteresis; (b) equivalent oxide thickness (t_{eq}) after annealing at 600 °C in O_2 vs $LaAlO_3$ thickness (t_{LAO}).

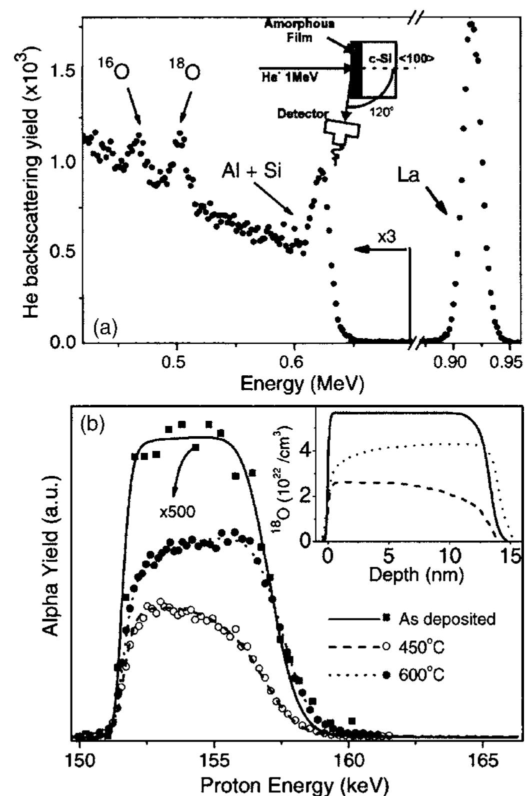

FIG. 2. (a) Channeled-RBS spectrum. Experimental geometry is sketched in the inset. (b) Excitation curves of the $^{18}O(p,\alpha)^{15}N$ nuclear reaction. Sample tilt 60 ° with the normal to the sample surface. The experimental curve for the as-deposited sample is multiplied by 500.

smaller influence on the capacitance at accumulation of the thicker 40 nm dielectric film as compared to the much thinner 5 nm thick dielectric. As a result, differences in the capacitance at accumulation are barely observed in the $C \times V$ curves for capacitors made up with 40 nm thick $LaAlO_3$ films. Figure 1(b) shows the capacitance equivalent to SiO_2 thickness (t_{eq})[1] versus $LaAlO_3$ thickness (t_{LAO}) for MOS capacitors after annealing in O_2 atmosphere at 600 °C. From the slope of the linear fit to the data in Fig. 1(b) it is possible to calculate the dielectric constant of the deposited $LaAlO_3$ films, excluding the effects of the lower-κ interfacial layer. The calculated dielectric constant was approximately 14, which is substantially lower than the dielectric constant of the bulk material. This may be attributed[13] to the lower density of the $LaAlO_3$ amorphous phase (5.5 g/cm^3 for this work) as compared to its crystalline phase (6.5 g/cm^3). Assuming that the molecular polarizability (α) is the same for both $LaAlO_3$ crystalline and amorphous phases and considering the Clausis Mossotti equation, $(\kappa-1)/(\kappa+2) = (4\pi/3)\ \alpha/V_{mol}$, a small increase of the molecular volume (V_{mol}), or in other words, a lower mass density effectively leads to a much larger reduction of the dielectric constant.

Extrapolating the t_{eq} versus t_{LAO} curve to $t_{LAO}=0$ gives a thickness of the lower-κ interfacial layer of about 4 nm. However, for the thicker $LaAlO_3$ films the intermediate layer may be thinner than 4 nm.

La, ^{16}O, and ^{18}O areal densities of as-deposited and $^{18}O_2$-annealed, 13 nm thick $LaAlO_3$ films were determined by Rutherford backscattering spectroscopy (RBS) of incident 1 MeV He^+ ions parallel to the ⟨100⟩ axis of the underlying Si substrate (channeled RBS), detected in grazing direction.[14–16] A typical channeled-RBS spectrum for an $^{18}O_2$-annealed sample is shown in Fig. 2(a). Since the Al signal overlaps the Si signal, the Al areal densities were independently determined by nuclear reaction analysis using the $^{27}Al(p,\gamma)^{28}Si$ nuclear reaction at 992 keV.[17] All areal densities are given in Table I. It also shows that thermal annealing in $^{18}O_2$ promotes exchange of ^{16}O atoms previously in the film for ^{18}O atoms from the gas phase.[18] Within experimental uncertainties, no net oxygen incorporation is observed after $^{18}O_2$ annealing at 450 °C of the 13 nm $LaAlO_3/Si$ sample, while 600 °C annealing promotes both ^{16}O–^{18}O exchange and net oxygen incorporation. In addition, no metal losses are observed.

Oxygen incorporation and interfacial layer formation during annealing were further inspected, by determining the ^{18}O profiles in 13 nm $LaAlO_3/Si$ samples. The ^{18}O profiles were determined by narrow resonance nuclear reaction profiling (NRP)[16] using the narrow ($\Gamma = 100$ eV) resonance at 151 keV in the cross section curve of the $^{18}O(p,\alpha)^{15}N$ nuclear reaction. Figure 2(b) shows the excitation curves of the $^{18}O(p,\alpha)^{15}N$ nuclear reaction near the resonance at 151

TABLE I. Areal densities of La, Al, ^{16}O, and ^{18}O as determined by Rutherford backscattering spectrometry and nuclear reaction analysis in 13 nm thick, as-deposited and $^{18}O_2$-annealed $LaAlO_3$ films on Si. Typical errors in the areal densities are 3% for La, 10% for Al, and 5% for ^{16}O and ^{18}O.

	Areal densities (10^{15} at/cm^2)				
Sample	La	Al	^{16}O	^{18}O	$^{16}O + ^{18}O$
As-deposited	24.1	24	74	—	74
450 °C	24.9	23	43	30	73
600 °C	24.4	26	29	57	86

Reuse of AIP Publishing content is subject to the terms at: https://publishing.aip.org/authors/rights-and-permissions. Download to IP: 143.54.44.137 On: Thu, 05 May 2016 13:27:08

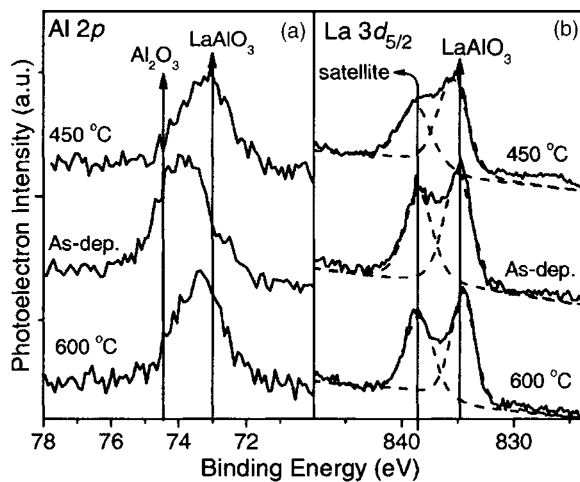

FIG. 3. (a) Al $2p$ and (b) La $3d_{5/2}$ x-ray photoelectron spectra regions from as-deposited and $^{18}O_2$-annealed $LaAlO_3/Si$ samples.

keV for as-deposited and $^{18}O_2$-annealed $LaAlO_3/Si$ samples. The corresponding ^{18}O profiles are shown in the inset. Since the natural abundance of ^{18}O is 0.2%, if the excitation curve for the as-deposited sample is multiplied by a factor of 500, the oxygen profile extracted from this enhanced excitation curve represents the total ($^{16}O+^{18}O$) oxygen profile in the as-deposited sample, thus indicating the energy position corresponding to oxygen at the original interface. The ^{18}O profile for the 13 nm $LaAlO_3/Si$ sample annealed at 450 °C reveals that oxygen from the gas phase was mainly incorporated in near surface and bulk regions, barely reaching the $LaAlO_3/Si$ interface. On the other hand, during annealing at 600 °C the propagating ^{18}O front reaches slightly beyond the original $LaAlO_3/Si$ interface. If these findings are considered together with the data in Table I, one can say that during annealing at 450 °C most ^{18}O is incorporated in the $LaAlO_3$ film in exchange for ^{16}O previously existing in the oxide, while during annealing at 600 °C, ^{18}O is partly incorporated in exchange for ^{16}O and partly to form an ^{18}O-containing interfacial layer. This enhanced oxygen incorporation in the interfacial region promoted by the annealing at 600 °C heals interfacial electronic traps, bringing as a result an enhancement in the reduction of the hysteresis and flat band voltage shift for the sample annealed at 600 °C as compared to the one annealed at 450 °C [see Fig. 1(a)].

Figure 3(a) shows the Al $2p$ and La $3d_{5/2}$ photoelectron regions from the as-deposited and annealed 13 nm thick $LaAlO_3$ films on Si, excited by a Mg Kα (1253.6 eV) x-ray source and measured at 30° takeoff angle. The binding energy was referenced assigning to the C $1s$ component from adventitious carbon 284.6 eV.[19] Since the samples were 13 nm thick films, the interface and substrate regions do not contribute significantly to the x-ray photoelectron spectra (XPS). One notices from Fig. 3(a) that both thermal annealings shifted the Al $2p$ component toward lower binding energy, closer to the expected binding energy of Al $2p$ electrons in $LaAlO_3$.[20] The small binding energy difference (less than 0.2 eV) of the Al $2p$ component for samples annealed at 450 and 600 °C may be attributed to uncertainties intrinsic to the charge referencing method.[19] The La $3d_{5/2}$ photoelectrons display two components, one at lower binding energy assigned to $LaAlO_3$ and a strong satellite component at higher binding energy. The latter can be assigned to photoemission followed by charge transfer from the valence band to the La $4f$ level which is characteristic of oxidized lanthanum species, such as La in $LaAlO_3$ or in La–(OH) which is probably formed in the surface region of the sample during air exposure.[21,22] Thermal annealing at 450 °C in $^{18}O_2$ reduced the FWHM of both La $3d_{5/2}$ components from typically 3.2 to 2.9 eV, while annealing at 600 °C promoted a further reduction of the FWHM to 2.7 eV. The FWHM reductions suggest reduction of the number of La configurations in the films, most probably because thermal annealing in oxygen atmosphere led to stoichiometry completion of the as-deposited, O-deficient $LaAlO_3$ compound film. Furthermore, it suggests also a reduction of differential charging after annealing.

In summary, postdeposition annealing of $LaAlO_3$ films on Si in O_2 atmosphere, at temperatures up to 600 °C, strongly reduces flat band voltage shift and $C\times V$ hysteresis of MOS capacitors. These improvements were associated with the reduction of oxide charge and interfacial density of electronic traps, owing to oxygen incorporation from the gas phase. Improvements brought about by 600 °C annealing as compared to 450 °C annealing can be a consequence of the fact that at 600 °C the propagating oxygen front reaches the interface, providing mobile oxygen to reduce oxygen deficiency in this particularly sensitive region.

The authors acknowledge the financial support provided by the Brazilian Agencies CAPES, CNPq, and FAPERGS.

[1]G. D. Wilk, R. M. Wallace, and. J. M. Anthony, J. Appl. Phys. **89**, 5243 (2001).
[2]I. A. Kingon, J. P. Maria, and S. K. Streiffer, Nature (London) **406**, 1032 (2000).
[3]M. Houssa, *High-k Dielectrics* (Institute of Physics, London, 2004).
[4]P. W. Peacock and J. Robertson, J. Appl. Phys. **92**, 4712 (2002).
[5]M. Copel, E. Cartier, and F. M. Ross, Appl. Phys. Lett. **78**, 1607 (2001).
[6]J.-P. Maria, D. Wicaksana, and A. I. Kingon, J. Appl. Phys. **90**, 3476 (2001).
[7]H. Nohira, T. Shiraishi, K. Takahashi, T. Hattori, I. Kashiwagi, C. Ohshima, S. Ohmi, H. Iwai, S. Joumori, K. Nakajima, M. Suzuki, and K. Kimura, Appl. Surf. Sci. **234**, 493 (2004).
[8]J. B. Cheng, A.-D. Li, Q.-Y. Shao, H.-Q. Ling, D. Wu, Y. Wang, Y.-J. Bao, M. Wang, Z-Q. Liu and N. B. Ming, Appl. Surf. Sci. **233**, 91 (2004).
[9]P. Sivasubramani, M. J. Kim, B. E. Gnade, R. M. Wallace, L. F. Edge and D. G. Schlom, H. S. Craft, and J.-P. Maria, Appl. Phys. Lett. **86**, 201901 (2005).
[10]K. J. Hubbard and D. G. Schlom, J. Mater. Res. **11**, 2757 (1996).
[11]B.-E. Park and H. Ishiwasra, Appl. Phys. Lett. **82**, 1197 (2003).
[12]H. Zhong, G. Heuss, and V. Misra, IEEE Electron Device Lett. **21**, 593 (2000).
[13]R. A. B. Devine, J. Appl. Phys. **93**, 9938 (2003).
[14]T. E. Jackman, J. R. MacDonald, L. C. Feldman, P. J. Silverman, and I. Stensgaard, Surf. Sci. **100**, 35 (1980).
[15]L. C. Feldman, P. J. Silverman, J. S. Williams, T. E. Jackman, and I. Stensgaard, Phys. Rev. Lett. **41**, 1396 (1978)
[16]I. J. R. Baumvol, Surf. Sci. Rep. **36**, 1 (1999), and references therein.
[17]M. Frank, Y. Chabal, M. L. Green, A. Delabie, B. Brijs, E. B. O. Da Rosa, I. J. R. Baumvol, and F. C. Stedile, Appl. Phys. Lett. **83**, 740 (2003).
[18]R. C. M. De Almeida, and I. J. R. Baumvol, Surf. Sci. Rep. **49**, 1 (2003).
[19]T. L. Barr and S. Seal, J. Vac. Sci. Technol. A **13**, 1239 (1995).
[20]C. D. Wagner, A. V. Naumkin, A. Kraut-Vass, J. W. Allison, C. J. Powell, and J. R. Rumble, Jr. (Eds.), *NIST Standard Reference Database 20, Version 3.4* (2003), available from ⟨http://srdata.nist.gov/xps/⟩.
[21]C. Suzuki, T. Mukoyama, J. Kawai, and H. Adachi, Phys. Rev. B **57**, 9507 (1998); L. Schlapbach and H. R. Scherrer, Solid State Commun. **41**, 893 (1982).
[22]L. F. Edge, D. G. Schlom, S. A. Chambers, E. Cicerrella, J. L. Freeouf, B. Holländer, and J. Schubert, Appl. Phys. Lett. **84**, 726 (2004).

Reuse of AIP Publishing content is subject to the terms at: https://publishing.aip.org/authors/rights-and-permissions. Download to IP: 143.54.44.137 On: Thu, 05 May 2016 13:27:08